21th International Conference on Renewable Energies and Power Quality (ICREPQ'23)
Madrid (Spain), 24th to 26th May 2023
Renewable Energy and Power Quality Journal (RE&PQJ)
ISSN 2172-038 X, Volume No.21, July 2023

Preliminary Identification of the Dynamics of a Floating Offshore Wind Turbine Barge

I. Galeote[1], S. Esteban[1] and M. Santos[2]

[1] Dept. of Computer Architecture and Automatics
Complutense University of Madrid
Faculty of Physics – Plaza de Ciencias, 1, 28040 Madrid (Spain)
Phone number: +0034 91 394 4534, e-mail: igaleote@ucm.es, sesteban@ucm.es

[2] Institute of Knowledge Engineering
Complutense University of Madrid
e-mail: msantos@ucm.es

Abstract. Offshore wind turbines have become an increasingly attractive source of renewable energy because of their potential to access and utilize energy from deeper waters with more stable, stronger winds. The goal of this paper is to propose a mathematical model based on transfer functions to identify and study the behavior of the six degrees of freedom of floating turbines. For this purpose, the system has been simulated with OpenFAST for specific environmental conditions. A subset of data has been used to identify transfer functions to obtain a control-oriented model. The model has been progressively validated, extending the preliminary proposed model. The scope and limitations of this methodology have been assessed, as well as the possibilities of extending the present work to include a more functional methodology oriented to system co-design.

Key words. Offshore Floating Wind Turbines, Linear Transfer Function, System Identification, Coupled Systems.

1. Introduction.

Floating offshore wind turbine (FOWT) technology is not as constrained by location as its onshore or coastal counterpart. This fact, together with the access to more stable and uniform offshore wind profiles, allows the development of higher power turbines, with plans for the introduction of generators up to 15 MW of power and 280 meters of nacelle height.

On the other hand, the remoteness of the operating sites and the complexity of the environment multiply the operation and maintenance (O&M) costs. Therefore, the industry's focus shifts to increasing the efficiency and longevity of the turbines, with the aim of minimizing said maintenance. One of the ways this can be achieved is through development of control systems which reduce vibrations that cut into the turbine's lifespan [1].

Consequently, it is important to develop turbine models that recreate and predict the behaviour of the six degrees of freedom of the system given a set of environmental conditions.

One of the major challenges that such a model has to face is to account for the effect of the multiple loads affecting the FOWT, which is difficult to model, since they are strongly coupled and highly nonlinear effects [2]. On the other hand, the simulation tools used to model these loads require large computational times [3].

Research aimed at modelling the dynamic behaviour of a floating turbine usually starts from a multiple tuned mass damper model, focusing the equilibrium point on the nacelle itself and considering the fore aft and side to side degrees of freedom [4]. In contrast, we will base our reference origin on the platform barge, and consider the six degrees of freedom associated with the non-stationary foundation.

To design a control system, a state space or transfer function model is more suitable to use than the mesh-type models, frequently used in computational fluid mechanics by means of finite volume calculations.

The aim of this work is to provide a simple, transfer function based, white box model of the system that allows control design. Moreover, the simplicity gives a physical interpretation of the model parameters that may be used for codesign.

2. Mathematical model.

The motion equations of a FOWT have many non-linear contributions: hydrodynamics, interactions with mooring lines, aerodynamic forces (both regular and irregular), seabed motions, ice loads… However, the main perturbation load of a floating wind turbine motion is the action of waves.

Initially, only wave and wind action are considered acting on the degrees of freedom of the system. We propose a dynamic model that depends only on the hydrodynamic properties of the platform and the elastic interactions between it and the mooring lines; and on a term of external forces caused by waves, wind and gravity (1).

$$\ddot{\boldsymbol{\xi}} - \boldsymbol{D}\dot{\boldsymbol{\xi}} - \boldsymbol{K}\boldsymbol{\xi} = \boldsymbol{F_k} \cdot \dot{\boldsymbol{\delta}} + \boldsymbol{F_d} \cdot \boldsymbol{\delta} + \boldsymbol{F_v} \cdot \dot{\boldsymbol{u}} + \boldsymbol{F_w} \cdot \boldsymbol{u} \quad (1)$$

Where:

- $\xi = [\boldsymbol{surge}, \boldsymbol{sway}, \boldsymbol{heave}, \boldsymbol{roll}, \boldsymbol{pitch}, \boldsymbol{yaw}]^{\boldsymbol{T}}$ is the state vector which contains the six spatial degrees of freedom of the system (Figure 1).

- $\boldsymbol{D}$ represents hydrodynamic damping, while $\boldsymbol{K}$ is the elastic response of the mooring lines and the hydrodynamic buoyancy.

- $\boldsymbol{\delta}$ is the wave elongation so that $\boldsymbol{F_d} \cdot \boldsymbol{\delta}$ **and** $\boldsymbol{F_k} \cdot \dot{\boldsymbol{\delta}}$ account for the external forces generated by the wave on the system. This last term captures a possible phase sift in the action of the force.

- $\boldsymbol{u}$ is the wind input, with its respective force coefficients analogous to those of the waves.

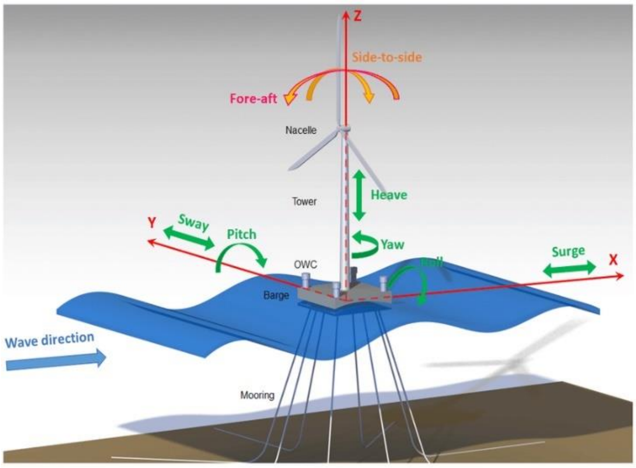

Figure 1. Spatial degrees of freedom of the FOWT.

Note the system corresponds to a damped harmonic oscillator with an external force, which is intended to capture the fundamental behaviour of the system.

It is important to take into account that here the rotational degrees of freedom are modelled as their translational counterparts, but an additional term that captures gyroscopic contributions must be considered. It has been shown that such a moment of force can stabilize the platform under certain operational conditions, reducing the effects of resonant frequencies [5].

Equation (1) can be transformed for each of the $\boldsymbol{\xi}$ components into six transfer functions, with two poles and a zero for each input (2).

$$\xi(s) = \frac{\boldsymbol{F_k} \cdot \boldsymbol{s} + \boldsymbol{F_d}}{\boldsymbol{s^2} - \boldsymbol{D} \cdot \boldsymbol{s} - \boldsymbol{K}} \cdot \boldsymbol{\delta}(\boldsymbol{s}) + \frac{\boldsymbol{F_v} \cdot \boldsymbol{s} + \boldsymbol{F_w}}{\boldsymbol{s^2} - \boldsymbol{D} \cdot \boldsymbol{s} - \boldsymbol{K}} \cdot \boldsymbol{u}(\boldsymbol{s}) \quad (2)$$

In order to consider waves not aligned with the axes, the angle of incidence α, defined as the angle between the direction of the wave and the x-axis, is introduced. This angle trigonometrically modulates the wave input to the surge and sway degrees of freedom, as seen in Figure 2. All simulations were carried out with α = 30º.

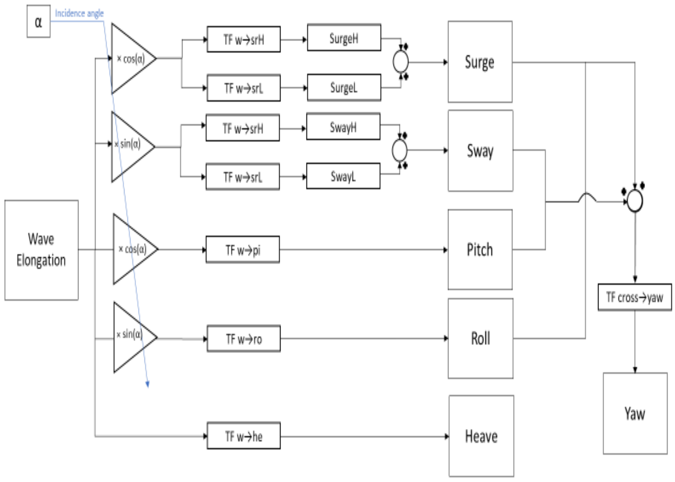

Figure 2. Wave to degrees of freedom diagram.

3. Simulation and Identification.

To develop the model, the OpenFAST simulation program, which allows to simulate a realistic and non-linear representation of these systems, was used to collect synthetic data used to identify the model parameters using MATLAB tools.

During this work, the system is excited with a modified developed wave spectrum (JONSWAP), which models a realistic sea state from two main parameters: Significant wave height $\boldsymbol{H_s}$, and peak spectral period $\boldsymbol{T_p}$.

The identification procedure is as follows: First, data are generated using OpenFAST and analysed. On certain windows of interest, a model identification is performed using MATLAB tools. Finally, the behaviour of the models is evaluated.

Because the MATLAB identification software prioritizes the steady state over the initial transient behaviour, the data generated by OpenFAST has been subdivided into identification data, on which the transfer function is calculated, and validation data, which is the complete data set.

The quality of the identification is measured by the normalized root mean square error (NRMSE) fit. Different identification improvement techniques will be discussed, prioritizing the maximization of the fit.

The chosen sea state for the identification is the sea state number (SSN) 6, which, as defined by [6], corresponds to $\boldsymbol{H_s} = \boldsymbol{4.88\,m}$, $\boldsymbol{T_p} = \boldsymbol{10.8\,s}$. Which is of considerable roughness, but not too extreme.

A. *Effect of the waves*

OpenFAST allows choosing in detail both the system input and whether or not to compute certain system loads.

Therefore, we excite the system with the discussed sea state conditions, but without the wind input, to isolate the hydrodynamic response of the system and thus allow a better study of it.

The synthetic data produced by OpenFAST are shown in Figure 3.

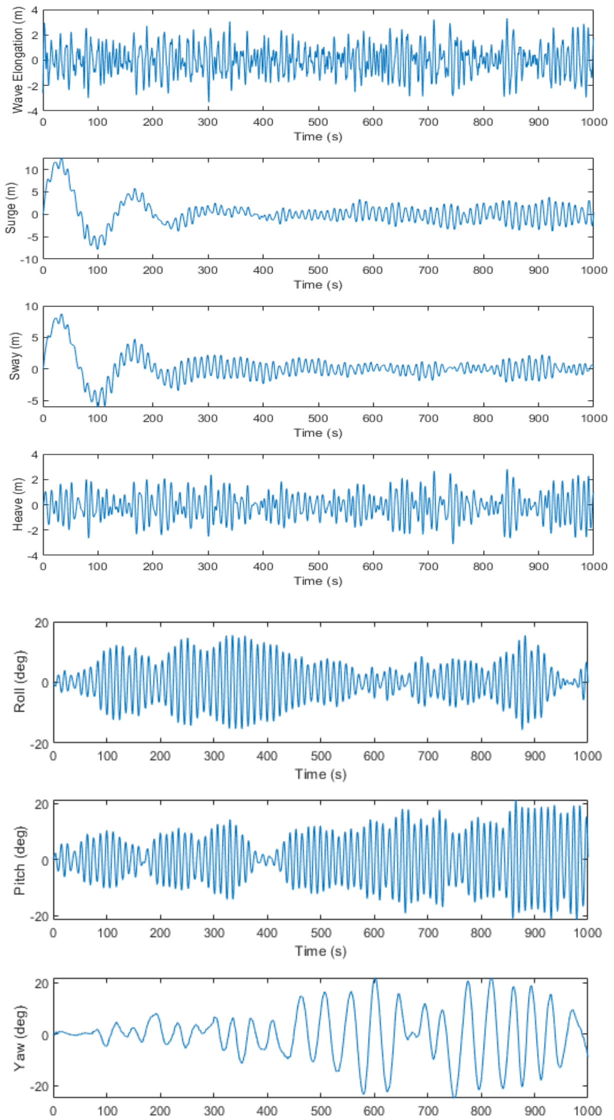

Figure 3. Incident wave and system degrees of freedom response under wave load.

As can be seen, the complete system contains multiple couplings and feedbacks that need to be accounted for in order to improve the identification of the six degrees of freedom.

A straightforward identification of data from Figure 3 gives a poor NMRSE fit, as shown in Figure 4.

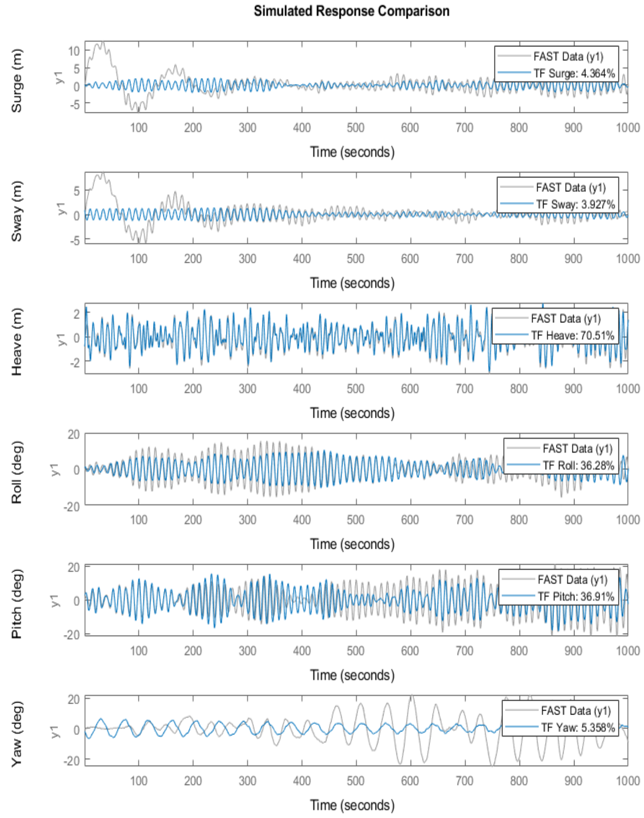

Figure 4. Preliminary identification under wave load.

We will now discuss the individual strategies that have been taken to improve the identification and conclude with a complete block diagram of the system.

1) Surge and sway: Surge and sway suffer from a horizon problem: the system tends to prioritize identifying the steady state, so it fails to identify the transient state.

   Because of this, to improve the identification it is sufficient to use as identification data for the transfer function the first half of the data and validate with the full set of data generated by FAST. By implementing this measure, the identification improves significantly with respect to the preliminary identification, up to 60 %.

   However, another option that can be contemplated to try to simultaneously consider both behaviors is to split the signal into the fast components of the main oscillation that ends up resulting from the steady state, and the slow component of the initial response of the system. This can be achieved by constructing a filter based on a rational transfer function that separates the components (Figure 5).

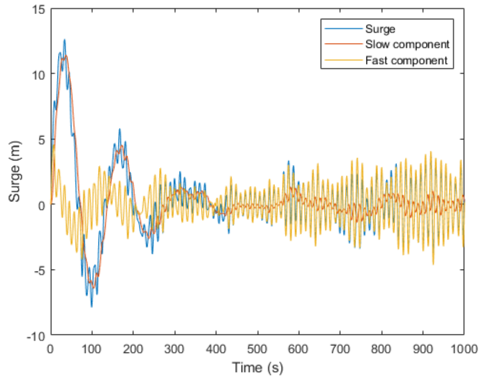

Figure 5. Frequency-filtered surge signal.

Next, each of the data subsets (high and low frequency components), are employed as the identification data for two transfer functions, with the lower frequency component capturing the behavior of the first half of the data, being an inherent response to the elastic dynamics of mooring; while the higher frequency behavior is present throughout the data set, as it its more closely related to the wave. Analogous action is taken for the sway.

Subsequently, the transfer functions are series coupled and finally validated with the full dataset, improving the identification in both transient and steady state (Figure 6).

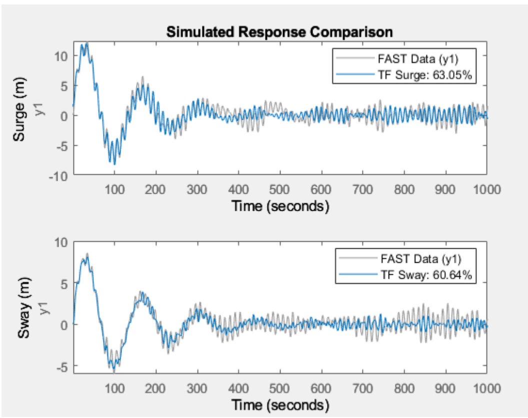

Figure 6. Improved identification of surge and sway.

2) Heave: The heave has a good identification fit, the result of responding directly to wave elongation, except for a delay in the force that is adequately captured in the transfer function.

3) Roll and pitch: To improve the identification of roll and pitch we can infer a relationship between the troughs of surge and sway with the first lobes of the x and y rotational modes.

This leads us to believe that the correct identification of these degrees of freedom is achieved by isolating the transient from the steady state.

However, partial identifications reveal that there does exist a transfer function that satisfactorily links the roll and pitch behavior to the wave input (Figure 7), but fails at the stages where destructive interference accumulates.

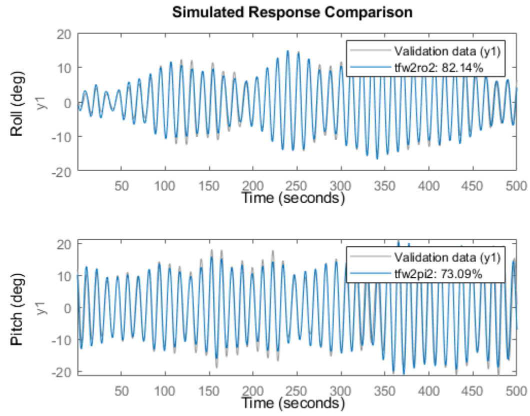

Figure 7. Selected improved identification of roll and pitch.

One way to implement this behavior in a potential future control system is to apply the control system only when a certain threshold is exceeded, at which point the system becomes predictable simply by knowing the wave profile.

4) Yaw: The yaw has a slow component that does not appear to be a direct product of the wave.

It is proposed that the combination of surge and roll generate a drag force on the barge. This displacement increases anchor line tension, generating a yaw-inducing overturn. Similarly, a similar effect occurs in the y axis with sway and pitch.

Therefore, a linear combination of surge modulated by the roll, and the sway modulated by the pitch is proposed as the new cross input, with the output being the yaw (3).

$$\text{cross} = \text{surge} \cdot \text{roll} + \text{sway} \cdot \text{pitch} \quad (3)$$

In Figure 8 it is verified that, indeed, the identification improves in the most relevant parameters in the analysis: An initial transient state where yaw hardly exists, followed by a slow oscillation with a period of destructive interference, to finally recover the slow oscillation, which has the desired frequency.

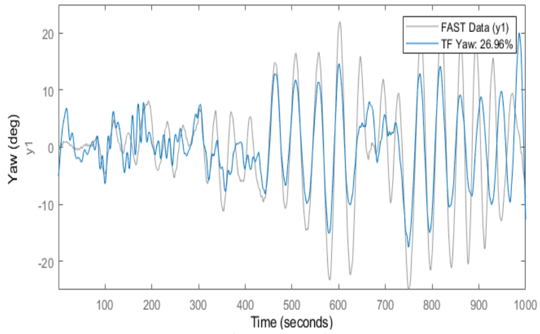

Figure 8. Improved identification of the yaw with cross input.

B. *Effect of the wind.*

Next, we discuss the contribution of the uniform wind input available in the OpenFAST environment.

Adding wind to our analysis has the additional effect of adding one more degree of freedom to the system, the motion of the rotor, and consequently, of the blades. This implies the appearance of gyroscopic effects as the rotations of the system interact.

Figure 9 shows the OpenFAST output after a simulation under the same sea state as the previous section, with a uniform wind of 8 m/s in the x direction.

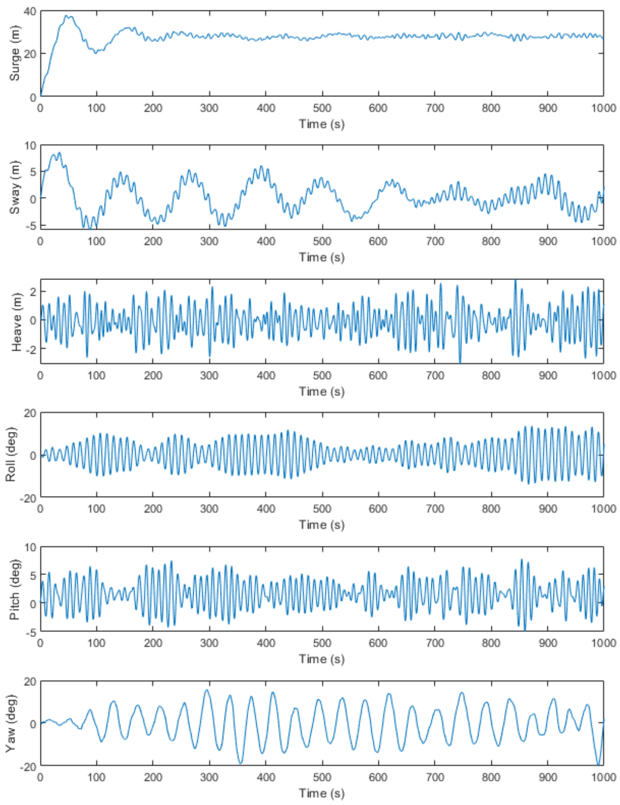

Figure 9. Responses of the six degrees of freedom to the simulation conditions SSN 6 and stable wind of 8 m/s.

As can be seen, the surge has been displaced in the positive direction of the x axis, performing a typical response of a second-order system to a step potential, with an overshoot, followed by a ringing or damping period, which disappears after a given stabilization time around an equilibrium position given by the length of the mooring line.

The sway behaves similarly to its windless counterpart, although the transient takes longer to stabilize, with a constructive interference stage around the end of the simulation.

Roll, pitch and yaw also respond similarly to the previous section, but with certain details that are better appreciated after identification.

We now proceed to configure the identification tool to accept two inputs and one output. The identification (Figure 9) yields an acceptable result, allowing us to assess with greater confidence the weight that the wind has on the system behaviour.

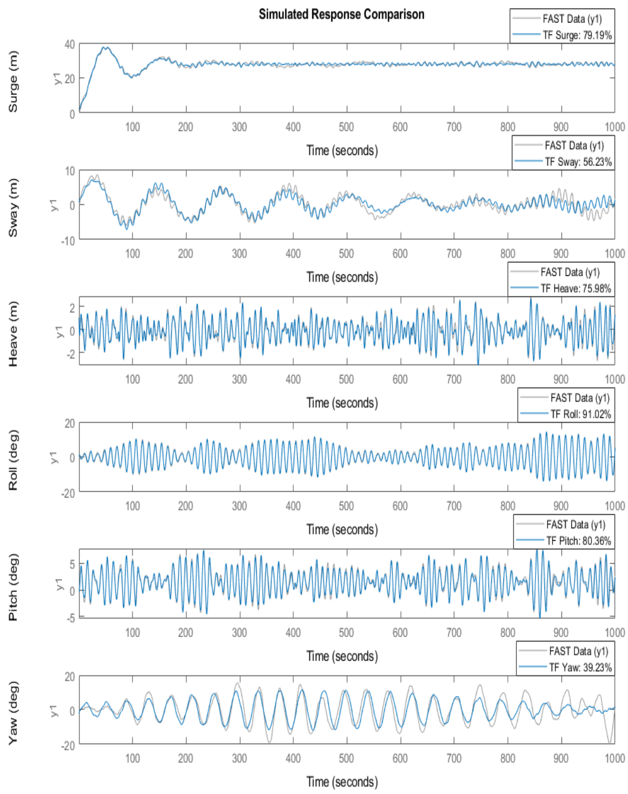

Figure 10. Identification of the six degrees of freedom with two inputs under wind a wave loads.

Figure 10 shows interesting results. All degrees of freedom have a good identification fit, but the way they do so is different for each case:

1) The surge is well coupled by the combination between the wind step function and the sinusoidal behaviour of the wave.

2) The pitch has a shift on its equilibrium point, since the wind turbine acts as a sail, so the potential step introduced by the wind allows to account for this new equilibrium point, which is around the designed static pitch of the platform.

3) The yaw gains smoothness in its identification, losing the peaks it had when taking the cross input on the wave-load only section. It is necessary to employ additional identification techniques to characterize this degree of freedom, such as adding a gyroscopic term to the system.

4. Conclusions and future work.

The behaviour of the different degrees of freedom of the FOWT under wave and wind loads has been observed, and the most common techniques to improve the predictive capability of the model have been discussed, operating always with transfer functions easy to implement in a control algorithm, under certain operational conditions.

Given the simplicity of the model, a considerably successful identification of the hydro-wind coupled response has been achieved.

As future work, an expansion of the wind profiles for various angles and turbulence is proposed, giving a more realistic picture of the limitations of this approach. This can also be extended to more severe sea states, where small angle approximations are not as suitable as before.

The model can also be extended to host more inputs, such as a gyroscopic contribution, ice effects, or second order elastic effects in tower twisting and stretching, which would be strongly nonlinear.

Acknowledgement.

This work has been partially supported by the Spanish Ministry of Science and Innovation under the MCI/AEI/FEDER project number PID2021-123543OB-C.

References.

[1] K. Tong. Technical and economic aspects of a floating offshore wind farm. *Journal of Wind Engineering and Industrial Aerodynamics*, 74:399–410, 1998.

[2] D. Matha, M. Schlipf, R. Pereira, and J. Jonkman. Challenges in simulation of aerodynamics, hydrodynamics, and mooring-line dynamics of floating offshore wind turbines. In *The twenty-first international offshore and polar engineering conference*. OnePetro, 2011.

[3] Y. Liu, S. Li, Q. Yi, and D. Chen. Developments in semi-submersible floating foundations supporting wind turbines: A comprehensive review. *Renewable and Sustainable Energy Reviews*, 60:433–449, 2016.

[4] Tomas-Rodriguez, M. & Santos, M. (2019). Modelling and control of floating offshore wind turbines. *Revista iberoamericana de automática e informatica industrial*, 16(4).

[5] S. Esteban, R. Lopez, M. Guijarro, and M. Santos. Gyroscopic effect on floating offshore wind turbines.

[6] S. C. Yim, T. Nakhata, and E. T. Huang. Coupled nonlinear barge motions, part II: Stochastic models and stability analysis. *J. Offshore Mech. Arct. Eng*., 127(2):83–95, 2005.